HOKKAIDO UNIVERSITY

| | |
|---|---|
| Title | An HCCI combustion engine system using on-board reformed gases of methanol with waste heat recovery : ignition control by hydrogen |
| Author(s) | Shudo, Toshio |
| Citation | International Journal of Vehicle Design, 41(1/2/3/4), 206-226<br>https://doi.org/10.1504/IJVD.2006.009669 |
| Issue Date | 2006 |
| Doc URL | https://hdl.handle.net/2115/30301 |
| Type | journal article |
| File Information | IJVD41.pdf |

Hokkaido University Collection of Scholarly and Academic Papers : HUSCAP

# An HCCI combustion engine system using on-board reformed gases of methanol with waste heat recovery: ignition control by hydrogen

Toshio Shudo

Division of Energy and Environmental Systems,
Hokkaido University, N13 W8 Kita-Ward, Sapporo 060-8628, Japan
Fax: +81-11-706-6402
E-mail: shudo@eng.hokudai.ac.jp

**Abstract:** Adjusting a proportion of two fuels with different ignition properties is an effective technique for controlling the ignition timing in HCCI combustion. This research newly proposes an HCCI combustion engine system fuelled with dimethyl ether (DME) having a high cetane number and methanol-reformed gas (MRG) having a high anti-knock property. In the system, both DME and MRG are to be produced from methanol by onboard reformers utilising the exhaust heat from the engine. Because the reactions producing DME and MRG are endothermic, a part of exhaust heat energy can be recovered during the fuel reforming process. This research experimentally investigated characteristics of combustion, exhaust emissions, engine efficiency and overall thermal efficiency including the waste heat recovery through the fuel reforming in the HCCI combustion engine system. Because MRG consists of hydrogen and carbon monoxide, effects of the two on the autoignition of DME were also analysed.

**Keywords:** DME; HCCI; hydrogen; ignition control; methanol; on-board reforming; waste heat recovery.

**Reference** to this paper should be made as follows: Shudo, T. (2006) `An HCCI combustion engine system using on-board reformed gases of methanol with waste heat recovery: ignition control by hydrogen', Int. J. Vehicle Design, Vol. 41, Nos. 1/2/3/4, pp.206-226.

**Biographical notes**: Toshio Shudo gained his BEng, MEng and DrEng degrees from Hokkaido University, Sapporo Japan. In 1995, he was a Researcher in the Engine Research Division, Mitsubishi Motors Co., Okazaki Japan. In 1997 he was Assistant Professor and from 2002, Associate Professor at the Musashi Institute of Technology, Tokyo Japan. In 2003, he was Visiting Scientist at the Massachusetts Institute of Technology, Cambridge MA, USA. In 2004 he was Professor at the Kitami Institute of Technology, Kitami Japan, and Associate Professor at Hokkaido University, Sapporo Japan from 2005. In 2000 he received the Asahara Memorial Academic Award from the Japan Society of Automotive Engineers, and in 2002, he received the Research Encouragement Award from the Japan Society of Mechanical Engineers.

## 1. Introduction

It is expected that the use of homogeneous charge compression ignition (HCCI) combustion in internal combustion engines will result in the higher thermal efficiency and the lower NOx emission as compared with conventional combustion systems. However, the difficulty in controlling the ignition timing in accordance with the engine load is preventing the HCCI combustion from its practical application to vehicles. Adjusting the proportion of two fuels with different ignition properties has been reported as a technique to control the ignition timing and load in HCCI combustion [1,2]. However, this technique has not been practically used for vehicles because of the obvious inconvenience of carrying two kinds of fuels onboard.

On the other hand, dimethyl ether (DME) has been studied as a clean alternative to the diesel fuel due to its high cetane number and smokeless combustion [3-5]. DME can be easily produced from methanol by the dehydration reaction [6]. There has been reported an idea to use a small amount of DME that was produced from methanol as an ignition improving agent in a methanol direct-injection diesel engine [3]. Methanol also can be thermally decomposed to methanol-reformed gas (MRG) that consists of hydrogen and carbon monoxide. Since both hydrogen and carbon monoxide have high anti-knock properties [7], MRG has been studied as a fuel for spark-ignition engines [8,9].

For this background, the author newly proposes an HCCI combustion engine system that is fuelled with DME and MRG. Because the ignition properties of DME and MRG are largely different, adjusting the proportion of the two fuels could control the ignition timing in the HCCI combustion engine fuelled with them. In addition to the ignition control, the author also proposes productions of DME and MRG by onboard methanol reformers utilising the exhaust gas heat of the HCCI engine as shown in Figure 1. Because the reactions to produce DME and MRG from methanol are endothermic, the produced DME and MRG have higher heating values than liquid methanol. Therefore, the methanol reformation using the engine exhaust gas heat can be a technique for recovering the waste heat from the engine. In addition to the high engine efficiency by HCCI operation, the waste heat recovery could achieve a high overall thermal efficiency in the system. The use of the single liquid fuel, methanol, also eliminates the obvious inconvenience of having to carry two fuels onboard and makes the HCCI combustion applicable to vehicles. In this research, characteristics of combustion, exhaust emissions and thermal efficiency were analysed in the HCCI combustion engine fuelled with DME and MRG. The experiments were conducted with varying the proportion of the fuels, the equivalence ratio and the compression ratio. The overall thermal efficiency including the waste heat recovery by the fuel reforming was also calculated for ideal cases. Because the MRG consists of hydrogen and carbon monoxide, this research also aimed to separate each influence of the two on the auto-ignition of DME.

## 2. Reforming Reactions and Tested Fuels

Dimethyl ether (DME; $CH_3OCH_3$) can be easily produced by the catalytic dehydration of methanol ($CH_3OH$) over a gamma-alumina catalyst [6].

$$CH_3OH \text{ (liquid)} \rightarrow 0.5CH_3OCH_3 + 0.5H_2O;\ \Delta H=25.9\text{kJ} \quad (1)$$

Because the above reaction is endothermic, the produced $0.5CH_3OCH_3$ has a 4% larger heating value than liquid $CH_3OH$. Methanol also can be thermally decomposed into 2mol of hydrogen and 1mol of carbon monoxide by the following reaction on an adequate catalyst.

$$CH_3OH \text{ (liquid)} \rightarrow 2H_2 + CO;\ \Delta H=128.5\text{kJ} \quad (2)$$

The $2H_2 + CO$ has a 20.1% higher heating value than the liquid $CH_3OH$. Therefore, the productions of DME and MRG from methanol using the heat of the engine exhaust gas can be a technique for recovering the waste heat. The experiments in this research used DME and an MRG model gas that consists of 67% hydrogen and 33% carbon monoxide by volume.

## 3. Experiments

The engine used in the experiments is a four-stroke cycle single-cylinder engine that has a bore of 85mm and a stroke of 88mm. The compression ratio was set at 8.3, 9.7, 12.4 and 15.8 by adjusting the height of a flat-shaped piston crown. The fuel gases, DME and the MRG model gas, stored in high-pressure cylinders were continuously supplied into the intake manifold of the engine. The flow rates of the two fuels were separately controlled using needle valves and measured by mass flow meters (Oval MASFLO-OVAL). The in-cylinder pressure was measured with a piezo-electric pressure-transducer (AVL GM12D) installed in the cylinder head as shown in Figure 2. For each experimental condition, the pressure data for 100 cycles were averaged and used to calculate the indicated mean effective pressure, the indicated thermal efficiency and the apparent rate of heat-release. The apparent rate of heat-release was used to calculate the degree of constant volume and the cooling loss fraction. The CO concentration in the exhaust gas was measured with an NDIR analyser, the THC concentration with an FID analyser, and the $O_2$ concentration with an MPA type analyser.

The engine speed was set at 1000 rpm for all the experiments. The volumetric efficiency was controlled by an intake throttle valve to keep a constant value of 75% including fuel gases for the better comparison of the thermal efficiency. The intake air was at a room temperature without heating.

## 4. Analysis of Thermal Efficiency

The indicated thermal efficiency $\eta_i$ of an internal combustion engine is expressed by Equation (3) using the theoretical thermal efficiency of the Otto cycle $\eta_{th}$, the degree of constant volume $\eta_{glh}$, the combustion efficiency $\eta_u$ and the cooling loss fraction $\phi_w$ [10].

$$\eta_i = \eta_{th}\eta_{glh}\eta_u(1-\phi_w) \tag{3}$$

This research evaluated the cooling loss fraction $\phi_w$ and the degree of constant volume $\eta_{glh}$ from the in-cylinder pressure diagram. The measured pressure is influenced by the cooling loss caused by the heat transfer from burning gas to the combustion chamber wall. The cumulative apparent heat-release $Q$, which is calculated from the measured pressure, is related to the cumulative real heat-release $Q_B$ and the cumulative cooling loss $Q_C$ as follows.

$$Q = Q_B - Q_C \tag{4}$$

The cooling loss fraction, which is defined as $\phi_w = Q_C/Q_B$, is written as follows.

$$\phi_w = (Q_B - Q)/Q_B \tag{5}$$

Because the $Q_B$ can be described with the combustion efficiency $\eta_u$ and the supplied fuel heat in a cycle $Q_{fuel}$, the cooling loss fraction $\phi_w$ can be rewritten with the following equation [11].

$$\phi_w = 1 - Q/(\eta_u Q_{fuel}) \tag{6}$$

The cumulative apparent heat-release $Q$ is obtained by integrating the apparent rate of heat-release $dQ/d\theta$ that is calculated with the in-cylinder volume $V$, the in-cylinder pressure $P$, the specific heat ratio $\gamma$ and the crank angle $\theta$ as follows.

$$dQ/d\theta = V/(\gamma-1)dP/d\theta + \gamma P/(\gamma-1)dV/d\theta - PV/(\gamma-1)^2 d\gamma/d\theta \tag{7}$$

Though the term with $d\gamma/d\theta$ in the above equation is often neglected by some researchers, it can be quite large during combustion of hydrogen due to its rapid changes in temperature and composition of the in-cylinder gas [12]. Considering the rapid combustion in HCCI engines, this research included the term to the calculation.

The degree of constant volume $\eta_{glh}$ is defined with the apparent rate of heat-release $dQ/d\theta$ by the following equation [10, 11].

$$\eta_{glh} = 1/(\eta_{th}Q)\int(1 - ((V_h + V_c)/V)^{1-\gamma})dQ/d\theta\, d\theta \tag{8}$$

where $V_h$ and $V_c$ are the stroke volume and the clearance volume of the engine respectively.

## 5. Results and Discussions

### 5.1 Influence of proportion of DME and MRG

Characteristics of the HCCI combustion engine that was fuelled with DME and MRG were analysed with varying the proportion of the two fuels. Figure 3 shows the influence of the fuel proportion on the indicated mean effective pressure IMEP, the indicated thermal efficiency $\eta_i$ and exhaust emissions in the HCCI combustion at the compression ratio of 9.7. The MRG fraction in the totally supplied fuel amount was set at 0, 40, 50 and 60% by volume. The figure indicates that a larger MRG fraction enables richer combustion and higher IMEP. The HCCI combustion of DME and MRG demonstrates quite high thermal efficiencies over a wider range of operable equivalence ratio and higher IMEP compared to that of the neat DME. The concentrations of THC and CO in the exhaust gas tend to decrease as the equivalence ratio $\phi$ increases. The adjusting the proportion of MRG and DME is very effective to expand the range of operable equivalence ratio in the HCCI combustion engine.

Figure 4 shows the indicator diagram of the HCCI combustion at the equivalence ratios that resulted in the highest thermal efficiency for each MRG fraction in the experiments in Figure 3. As shown in Figure 4, the optimum equivalence ratio tends to increase as the MRG fraction increases. Each diagram has a two-stage heat-release with the first-stage by the low-temperature oxidation and the second-stage by the high-temperature oxidation, which is typical for the HCCI combustion of DME. It is clear that the MRG fraction can effectively control the heat-release in the HCCI combustion of DME and MRG. While the first heat-release is hardly influenced by the MRG fraction, the second heat-release is remarkably influenced by the fraction. An increased MRG fraction retards the beginning of the second heat-release that is the main heat-release in the HCCI combustion. The retarded main heat-release avoids a too early combustion phase and a too high pressure-rise in spite of the increased equivalence ratio. These are the reasons for the extension of the operable equivalence ratio range by the MRG addition to the HCCI combustion of DME shown in Figure 3.

### 5.2 Influence of compression ratio

Figure 5 shows characteristics of the HCCI combustion of DME and MRG for different compression ratios. The compression ratio $\varepsilon$ was set at 8.3, 9.7, 12.4 and 15.8. Here, combustion limits on the richer mixture side were set by the maximum rate of pressure rise of 300kPa/°CA. The range of operable equivalence ratio shifts to the richer mixture side as the compression ratio decreases. The compression ratio of 9.7 resulted in the highest indicated thermal efficiency among the four ratios. A lower compression ratio allows richer combustion with higher IMEP and lower exhaust emissions. The results also suggest a possibility of an ignition control by adjusting the compression ratio in an HCCI combustion engine. Figure 6 shows the indicator diagrams for the each compression ratio. The MRG fraction and the equivalence ratio were set at optimum values for the thermal efficiency. A lower compression ratio retards the beginnings of the both heat-releases by the low- and the high-temperature oxidation. The optimum equivalence ratio increases as the compression

ratio decreases, because the retarded heat-release enables richer combustion without causing the too early combustion phase. This is the reason for the higher power output at lower compression ratios in Figure 5.
Figure 7 shows the influence of compression ratio on the factors influencing the thermal efficiency such as the degree of constant volume and the cooling loss fraction. The MRG fraction was set at 60% by volume and the equivalence ratio was at optimum for the indicated thermal efficiency. The theoretical thermal efficiency $\eta_{th}$ was calculated with the each compression ratio ε and the specific heat ratio of 1.4 for the Otto cycle. The cooling loss fraction $\phi_w$ was obtained by Equation (6) using the combustion efficiency $\eta_u$ estimated by the measured oxygen concentration in the exhaust gas. The indicated thermal efficiency $\eta_i$ is decreased by an increased cooling loss fraction $\phi_w$ for compression ratios higher than 9.7 and by a decreased theoretical thermal efficiency $\eta_{th}$ for compression ratios lower than 9.7. Here, there is no significant change in the degree of constant volume $\eta_{glh}$, accordingly the trend of the indicated thermal efficiency $\eta_i$ is dominated mainly by the theoretical thermal efficiency $\eta_{th}$ and the cooling loss fraction $\phi_w$.

**5.3 Comparison of HCCI and SI**

Figure 8 shows a comparison of the HCCI and the homogeneous charge spark-ignition (SI) combustion at the compression ratio of 9.7. Because of the necessity for a high anti-knock property, the SI combustion was fuelled with neat MRG. Ignition was provided by a spark discharge in the central position of the combustion chamber, and set at the optimum timings for the indicated thermal efficiency. The thermal efficiency of the HCCI combustion is significantly higher than that of the SI combustion in leaner mixture conditions. Because of the high thermal efficiency, the HCCI combustion has a high power output that is comparable to the SI combustion in spite of the lean mixture condition. The HCCI combustion with the excess air ratios lower than 4.0 bring quite low CO exhaust emissions which are similar to the values in the SI combustion case. Although the THC exhaust emission from the HCCI combustion is higher than that from the SI combustion, the emission tends to decrease as the excess air ratio decreases. The THC emission could be after-treated by an oxidation catalyst in the practical use of the HCCI combustion engine system.
Figure 9 shows a comparison of the HCCI and the SI for the four different compression ratios. The results are plotted against the fraction of DME to the totally supplied fuel. The excess air ratio was set at the optimal for the indicated thermal efficiency at the each compression ratio and the DME fraction. The highest compression ratio brings the highest thermal efficiency in the SI combustion. Contrary to this, the HCCI combustion exhibits the highest thermal efficiency at the relatively low compression ratio of 9.7 over a wide range of the DME fraction. The thermal efficiency of the HCCI combustion is significantly larger than that of the SI combustion. The compression ratios of 8.3 and 9.7 bring higher IMEP in the HCCI combustion compared to the higher compression ratios. The level of the IMEP is comparable to that of the SI combustion of MRG. Though the HCCI combustion tends to emit higher THC and CO as compared with the SI combustion, the CO emissions from the HCCI combustion at the compression ratios of 8.3 and 9.7 are lower than those at the higher compression ratios.

**5.4 Overall thermal efficiency including waste heat recovery by fuel reforming**

As described in Section 2, DME ($CH_3OCH_3$) and MRG ($2H_2$+CO), which are produced from methanol, have the higher heating values compared to the liquid methanol. The utilisation of the engine exhaust gas heat for the endothermic reforming reactions can be a technique to recover the waste heat from the engine. This research introduces an index $\eta_r$ to express the degree of the increase in the heating value by the fuel reforming. The value of the index $\eta_r$ is calculated for the productions of DME and MRG with following equations respectively.

$$\eta_{r\,DME} = 0.5LHV_{CH3OCH3}/LHV_{CH3OH(l)} \quad (9)$$

$$\eta_{r\,MRG} = (2LHV_{H2} + LHV_{CO})/LHV_{CH3OH(l)} \quad (10)$$

The value is 1.04 for the neat DME production and 1.20 for the neat MRG production. The degree of heat increase for the each experimental condition is calculated by Equation (11).

$$\eta_r = \eta_{r\,DME}\,[DME]/([DME][MRG]) + \eta_{r\,MRG}\,[MRG]/([DME][MRG]) \quad (11)$$

Here, [DME] and [MRG] are fractions of DME and MRG to the totally supplied fuel in the experiments. Multiplying the degree of heat increase $\eta_r$ by the engine efficiency $\eta_i$ makes the overall thermal efficiency of the system including the waste heat recovery effect by the fuel reforming using the engine exhaust gas.

$$\eta_{overall} = \eta_r \eta_i \quad (12)$$

Figure 10 shows the overall thermal efficiency based on the LHV of liquid methanol for the results of HCCI and SI combustion under various operational conditions shown in Figure 8. Because the degree of heat increase $\eta_r$ is higher for the MRG production compared with the DME production, conditions with a larger amount of MRG have advantages in terms of the exhaust heat recovery. The SI combustion, which is fuelled with the neat MRG, has the higher waste heat recovery effect than the HCCI combustion of DME and MRG. However, the overall efficiency $\eta_r \eta_i$ of the HCCI combustion is higher than that of SI combustion, because of the very high engine efficiency by the HCCI operation and the effective exhaust heat recovery. Therefore, it is suggested that the newly proposed HCCI combustion engine system with the waste heat recovery by the onboard fuel reforming is an efficient and clean energy system. The use of the single liquid fuel, methanol, also eliminates the inconvenience of having to carry two fuels onboard while maintaining the effective ignition control by the combination of two fuels with different ignition properties.

**5.5 Ignition control effects by hydrogen and carbon monoxide**

While MRG shows the high effect of the ignition control in the HCCI combustion, it consists of hydrogen and carbon monoxide. This section tries to separate each influence of the two on the auto-ignition of DME. Figure 11 shows the effects of adding MRG, hydrogen or carbon monoxide to HCCI combustion of DME. The overall equivalence ratio was set at $\phi$=0.36, the fraction of DME in the totally supplied fuels was at 50% by volume. The hydrogen addition exhibits the largest effect of retarding the phase of the second heat-release by the high-temperature oxidation reactions. Figure 12 shows the influences of adding the ignition-controlling fuels on the crank angles of onsets of the first heat-release by the low-temperature oxidation reactions $\theta_{LTR}$ and those of the second heat-release by the high-temperature oxidation reactions $\theta_{HTR}$. Here, the hydrogen addition cases have slightly lower supplied fuel heats than the cases with carbon monoxide due to the difference in their volumetric heating-values. However, the difference is quite small as 1.8% at most in the cases of 40% DME fraction. An increase in the amount of any of the ignition-controlling fuels slightly retards the onset of the first heat-release $\theta_{LTR}$ and largely retards the onset of the second heat-release $\theta_{HTR}$. It is clear that hydrogen is more effective to control the phase of the second heat-release in the HCCI combustion of DME than carbon monoxide. Therefore, the ignition control effect by the MRG addition to the HCCI combustion of DME is mostly attributed to the effect of hydrogen.
The above results can be also influenced by a decrease in DME amount with increasing in the ignition-controlling fuels, since the

equivalence ratio is set at constant. The next section will compare the effects at constant DME amounts.

**5.6 Ignition control effects at constant DME amounts**

Figure 13 shows the indicator diagrams for HCCI combustion of DME with the additions of hydrogen or carbon monoxide at a constant DME amount. The DME amount was fixed at a value that brings the equivalence ratio of 0.27 at the 100% DME fraction. The fraction of hydrogen or carbon monoxide in the totally supplied fuels was varied from 0 to 60% by volume. The equivalence ratios calculated by the totally supplied fuels, which increase by the addition of hydrogen or carbon monoxide, are indicated in the figures. Figure 14 shows a comparison of the results with hydrogen and carbon monoxide at the 40% DME fraction. Figure 15 shows the crank angles at the onsets of the heat-releases by the low- and the high-temperature oxidation reactions ($\theta_{LTR}$, $\theta_{HTR}$), the in-cylinder gas mean temperatures at the timings ($T_{LTR}$, $T_{HTR}$) and the cumulative apparent heat-releases during the low- and the high-temperature oxidation reactions ($Q_{LTR}$, $Q_{HTR}$). These values are derived from the results in Figure 13.

The figures show that the addition of hydrogen or carbon monoxide retards the combustion phase in spite of the increased equivalence ratio, and the effect is clearly larger in the hydrogen addition. Though the hydrogen addition largely retards the timing of the second heat-release, there is no remarkable change in the temperature at the timing. Hydrogen also makes the first heat-release slower and effectively delays the temperature-rise during the low-temperature oxidation of DME. Because of the delayed temperature-rise, the starting-crank-angle of the second heat-release is largely retarded in spite of the no remarkable change in the starting-temperature of the high-temperature oxidation reactions. There is almost no change in the cumulative apparent heat-release during the low-temperature oxidation $Q_{LTR}$, while the heat release during the high-temperature oxidation $Q_{HTR}$ increases with the equivalence ratio.

**5.7 Reaction mechanism of ignition control**

The results in the previous sections show that the addition of hydrogen or carbon monoxide to the HCCI combustion of DME effectively retards the main heat-release by the high-temperature oxidation reactions. The reaction mechanism in the ignition control is discussed in this section.

The chemical kinetics mechanism by Curran, et al. [13] is sometimes used to describe the oxidation process of DME, and this mechanism is consistent with previous engine experiments [14]. The first step of the mechanism is the production of $CH_3OCH_2$ from DME. Though the initiation reaction is the H abstraction from DME by oxygen, the largest part of $CH_3OCH_2$ is produced by the following H abstraction reaction by OH in the low-temperature oxidation of DME [15].

$$CH_3OCH_3 + OH \rightarrow CH_3OCH_2 + H_2O \quad (13)$$

The $CH_3OCH_2$ reacts with $O_2$ or the third body to produce HCHO, OH and other species. The produced HCHO consumes OH in the following reaction.

$$HCHO + OH \rightarrow CHO + H_2O \quad (14)$$

The OH is the chain carrier in the low-temperature oxidation. As a result of productions and consumption of the OH, when d[OH]/d$t$ turns negative the chain branching terminates [16]. When hydrogen and carbon monoxide are introduced to this low-temperature oxidation process of DME, they supposedly consume OH in the following reactions.

$$H_2 + OH \rightarrow H_2O + H \quad (15)$$

$$CO + OH \rightarrow CO_2 + H \quad (16)$$

Reaction (15) is known to have a relatively large rate even at a low temperature [17]. The H produced from the reactions quickly recombines with $O_2$ to produce $HO_2$ then $HO_2$ reacts with H and produces $H_2O_2$. However, $HO_2$ and $H_2O_2$ are much less reactive than OH during the low-temperature oxidation process [18].

$$H + O_2 + M \rightarrow HO_2 + M \quad (17)$$

$$HO_2 + H \rightarrow H_2O_2 \quad (18)$$

The largely retarded low-temperature oxidation by the addition of hydrogen in this research can be attributed to the consumption of OH by hydrogen. The consumption reduces OH concentration and d[OH]/d$t$. This retards the H abstraction from $CH_3OCH_3$ by OH that is the main reaction in the first step of the oxidation of DME. Subsequently, this delays the heat-release and the temperature-rise during the low-temperature oxidation. While hydrogen does not affect the starting-temperature of the high-temperature oxidation reactions, the onset of the second heat-release delays due to the delayed temperature-rise.

Hydrogen, which largely influences the low-temperature oxidation reactions of DME, is a very effective ignition-controller for HCCI combustion engines fuelled with DME. Adjusting the proportion of hydrogen and DME can maintain adequate timings of the second heat-release without causing the too high rate of pressure-rise in HCCI operations at higher equivalence ratios.

**6. Conclusions**

This research newly proposed an HCCI engine system fuelled with DME and MRG (methanol-reformed gas; $2H_2 + CO$) that are produced from methanol by onboard reformer utilising the heat of the engine exhaust gas. Characteristics of combustion, exhaust emissions, operational range, heat recovery effect by onboard fuel reforming, ignition control effect and reaction mechanism in the system were analysed. Results derived from the research are as follows:

1. The ignition timing is effectively controlled in the HCCI combustion engine system fuelled with DME and MRG by adjusting the proportion of the two fuels. The controlled ignition enables an efficient HCCI operation at a wider range of the equivalence ratio and the engine load compared with the HCCI combustion of neat DME.
2. An increased compression ratio advances the onsets of both the first and the second heat-releases. The advanced ignition timings bring earlier combustion phases and increase the cooling loss by the heat transfer from the burning gas to the combustion chamber wall. The optimum compression ratio for thermal efficiency is relatively low as around 10 in the HCCI combustion of DME and MRG. By choosing the optimum compression ratio and proportion of DME and MRG, the HCCI combustion achieves a higher thermal efficiency and a comparable power output as compared with SI combustion fuelled with MRG.
3. An onboard reforming of methanol to produce DME and MRG by utilising the heat of the engine exhaust-gas can be a technique to recover the waste heat and to achieve a quite high overall thermal efficiency in the system. The use of the single liquid fuel, methanol, also eliminates the inconvenience of having to carry two fuels onboard while maintaining the effective ignition control by the combination of two fuels with different ignition properties.
4. Both hydrogen and carbon monoxide that are contained in MRG have effects to retard the beginning of the second heat-release in HCCI combustion of DME. The effect is far larger in the hydrogen addition compared to the carbon monoxide addition. Hydrogen is a very effective ignition controller for HCCI combustion engines fuelled with DME. Adjusting the proportion of hydrogen and DME can

maintain adequate timings of the second heat-release without causing the too high rate of pressure-rise in HCCI operations at higher equivalence ratios. The ignition control effect by the addition of MRG ($2H_2$+CO) to HCCI combustion of DME is mostly attributed to the effect of hydrogen.

5. Hydrogen makes the first heat-release slower and effectively delays the temperature-rise during the low-temperature oxidation of DME. Because of the delayed temperature-rise, the starting-crank-angle of the second heat-release is largely retarded in spite of the no remarkable change in the starting-temperature of the high-temperature oxidation reactions. The low-temperature oxidation is supposedly retarded by the consumption of OH radical by hydrogen. Because the H abstraction from DME by OH radical is the main reaction to produce $CH_3OCH_2$ in the low-temperature oxidation of DME, the reduced OH concentration effectively retards the early stage of DME oxidation.

**Acknowledgement**
The author would like to thank Mr. Yoshitaka Ono and Mr. Takehiro Takahashi, former students of the Musashi Institute of Technology, for their help in the research. This research was financially supported in part by the RC193 of the Japan Society of Mechanical Engineers.

**References**

1. Furutani, T., et al., A Ultra-Lean Premixed Compression-Ignition Engine Concept and its Characteristics, Proc. COMODIA 98, 1998.
2. Olsson, J., et al., Closed-loop control of an HCCI engine, SAE Paper 2001-01-1031, 2001.
3. Murayama, T., et al., A Study of Compression Ignition Methanol Engine with Converted Dimethyl Ether as an Ignition Improver, SAE Paper 922212, 1992.
4. Sorenson, S.C., et al., Performance and Emissions of a 0.273 Liter Direct Injection Diesel Engine Fuelled with Neat Dimethyl Ether, SAE Paper 950064, 1995.
5. Kajitani, S., et al., Engine Performance and Exhaust Characteristics of Direct-Injection Diesel Engine Operated with DME, SAE Paper 972973, 1997.
6. Bercic, G., et al., Catalytic Dehydration of Methanol to Dimethyl Ether Kinetic Investigation and Reactor Simulation, *Industrial & Engineering Chemistry Research*, 32, 1993.
7. Obert, E.F., *Internal Combustion Engines and Air Pollution*, Harper & Row, 1973.
8. Hirota, T., Study of Methanol-reformed Gas Engine, *J. SAE Japan*, 34-10, 1980.
9. Shudo, T., et al., Combustion Characteristics of $H_2$-CO-$CO_2$ Mixture in an IC Engine, *SAE Trans. J. Engines*, 110-3, 2002.
10. List, H. *Thermodynamik der Verbrennungskraftmaschinen*, Springer, 1939.
11. Shudo, T., et al., Analysis of the Degree of Constant Volume and Cooling Loss in a Spark Ignition Engine Fuelled with Hydrogen, *Int. J. Engine Research*, 2-1, 2001.
12. Shudo, T., et al., Influence of Specific Heats on Indicator Diagram Analysis in a Hydrogen-fuelled SI Engine, *JSAE Review*, 22-2, 2001.
13. Curran, H. J., et al., A Wide Range Modelling Study of Dimethyl Ether Oxidation, 26th Int. Symp. Comb., 1996.
14. Koyama, T., et al., Numerical Calculation of the Ignition and the Combustion in Homogeneous Charge Compression Ignition engine by using an Elementary Reaction Model in Case of Dimethyl Ether, *Trans. Japan Soc. Mech. Eng.* 67-657, B, 2001, (in Japanese).
15. Yamada, H., et al., A Study of Low Temperature Oxidation in Engine Using Quadrupole Mass Spectrometer, Proc. SAE Japan, 98-01, 2001, (in Japanese).
16. Yamada, H., et al., Chain Reaction Mechanism in Homogeneous Charge Compression Ignition of Dimethyl Ether, Abst. WIP, Int. Symp. Comb., 4-12-1423, 2002.
17. Jost, W., *Low Temperature Oxidation*, Gordon and Breach Science Publishers, 1965.
18. Eng, J.A., et al., The Effect of POx on the Autoignition Chemistry of n-Heptane in an HCCI Engine, Proc. SAE Japan, 25-02, 2002.

**NOMENCLATURE**

| | |
|---|---|
| HCCI | Homogeneous charge compression ignition |
| SI | Spark ignition |
| DME | Dimethyl ether |
| MRG | Methanol-reformed gas (67% $H_2$ + 33% CO) |
| IMEP | Indicated mean effective pressure |
| LHV | Lower heating value |
| $\Delta H$ | Enthalpy |
| THC | Total hydrocarbon |
| CA | Crank angle |
| ATDC | After top dead centre |
| $\varepsilon$ | Compression ratio |
| $\phi$ | Equivalence ratio |
| $\lambda$ | Excess air ratio |
| $\gamma$ | Specific-heat ratio |
| $\theta$ | Crank angle |
| $P$ | In-cylinder pressure |
| $V$ | In-cylinder volume |
| $V_h$ | Stroke volume |
| $V_c$ | Clearance volume |
| $dP/d\theta$ | Rate of pressure rise |
| $dQ/d\theta$ | Apparent rate of heat-release |
| $Q$ | Cumulative apparent heat-release |
| $Q_{fuel}$ | Supplied fuel heat per cycle |

$Q_B$ Cumulative real heat-release
$Q_C$ Cumulative cooling-loss
$\phi_w$ Cooling-loss fraction, $Q_C/Q_B$
$\eta_u$ Combustion efficiency
$\eta_i$ Indicated thermal efficiency
$\eta_{th}$ Theoretical thermal efficiency of Otto cycle, $\eta_{th}=1-\varepsilon^{1-\gamma}$
$\eta_{glh}$ Degree of constant volume
$\eta_r$ Degree of fuel heat increase in fuel reforming
$T_g$ In-cylinder mean gas-temperature
LTR Low-temperature oxidation reactions
HTR High-temperature oxidation reactions
$T_{LTR}$ Mean gas-temperature at beginning of LTR
$T_{HTR}$ Mean gas-temperature at beginning of HTR
$\theta_{LTR}$ Crank angle at beginning of LTR
$\theta_{HTR}$ Crank angle at beginning of HTR
$Q_{LTR}$ Cumulative apparent heat-release during LTR
$Q_{HTR}$ Cumulative apparent heat-release during HTR
MFC Mass flow controller

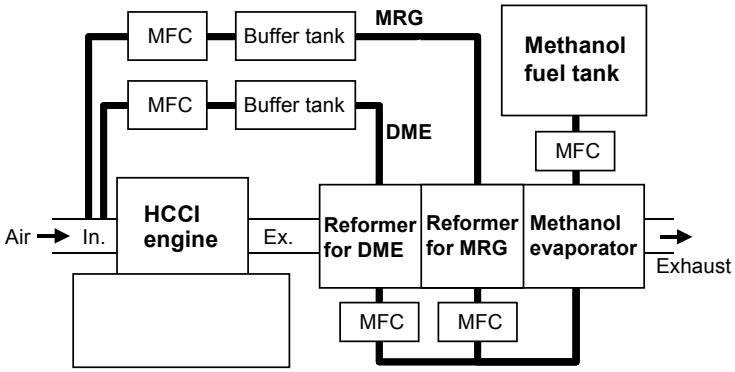


Fig.1 Proposed system of HCCI combustion engine fuelled with DME and MRG onboard-reformed from methanol.

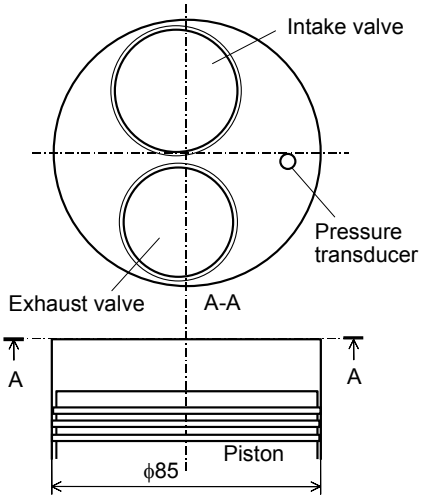


Fig.2 Combustion chamber of tested engine.

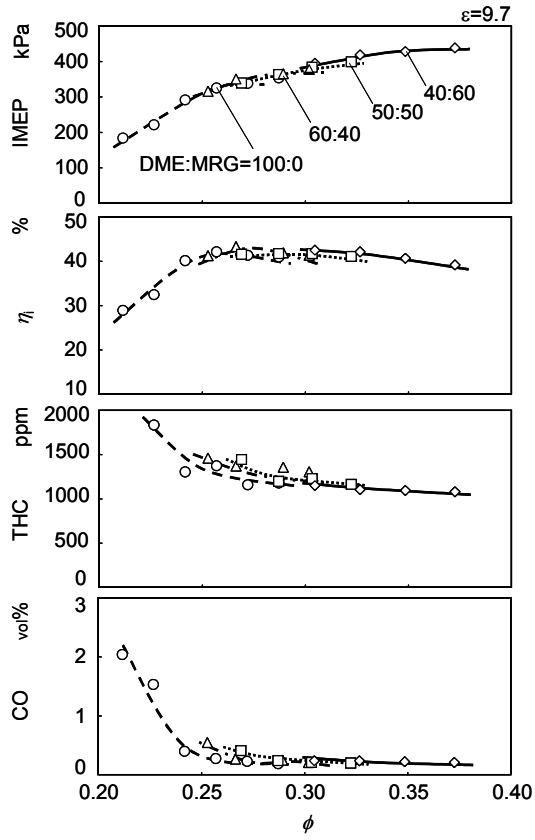


Fig.3 Indicated mean effective pressure, indicated thermal efficiency and exhaust emissions in HCCI combustion of DME and MRG.

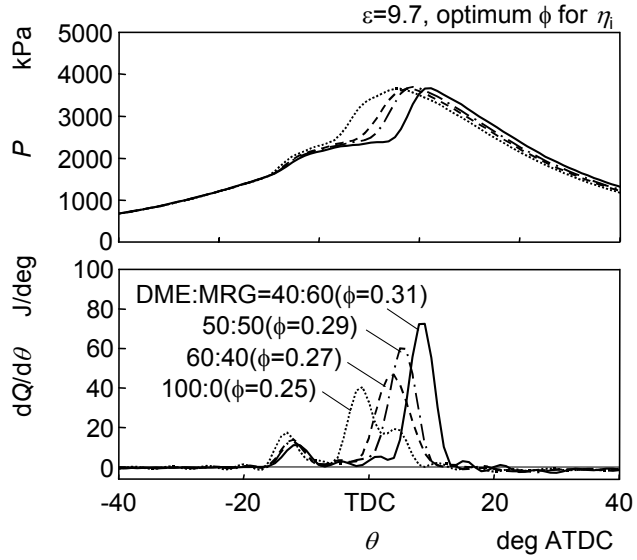


Fig.4 Indicator diagrams of HCCI combustion of DME and MRG.

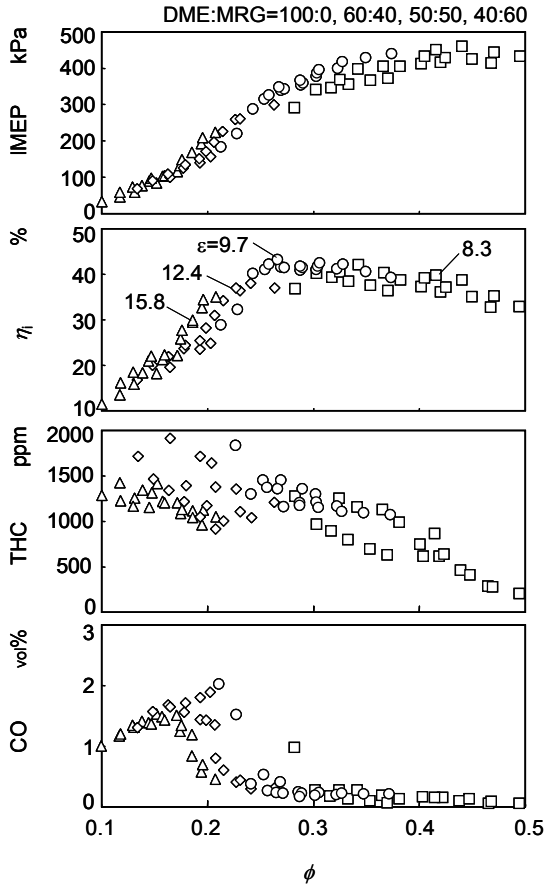


Fig.5 HCCI combustion of DME and MRG for different compression ratios (DME:MRG=100:0,60:40,50:50,40:60).

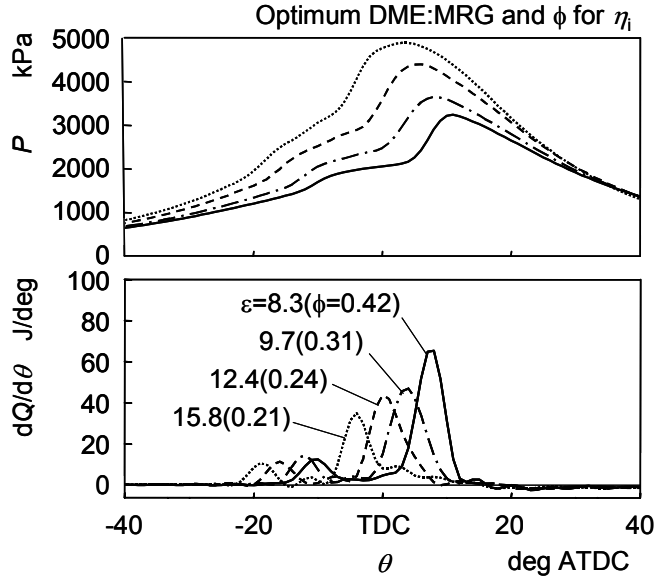


Fig.6 Indicator diagram of HCCI combustion for different compression ratios.

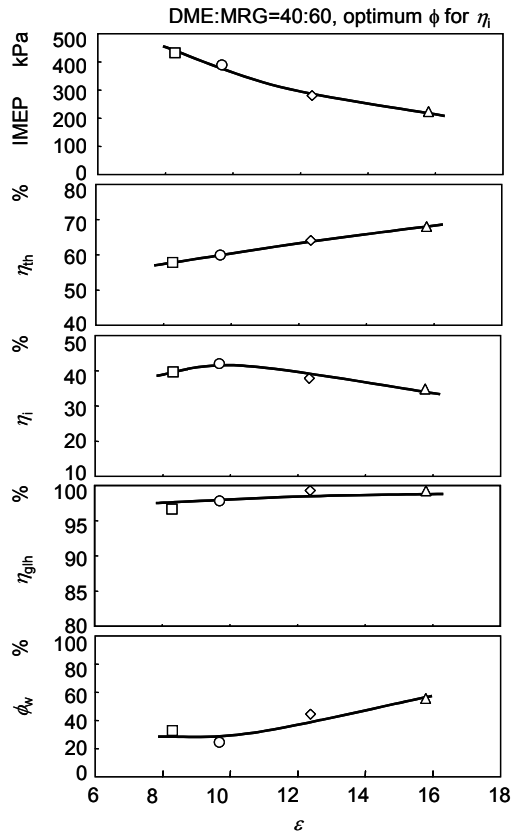


Fig.7 Influence of compression ratio on thermal efficiency factors.

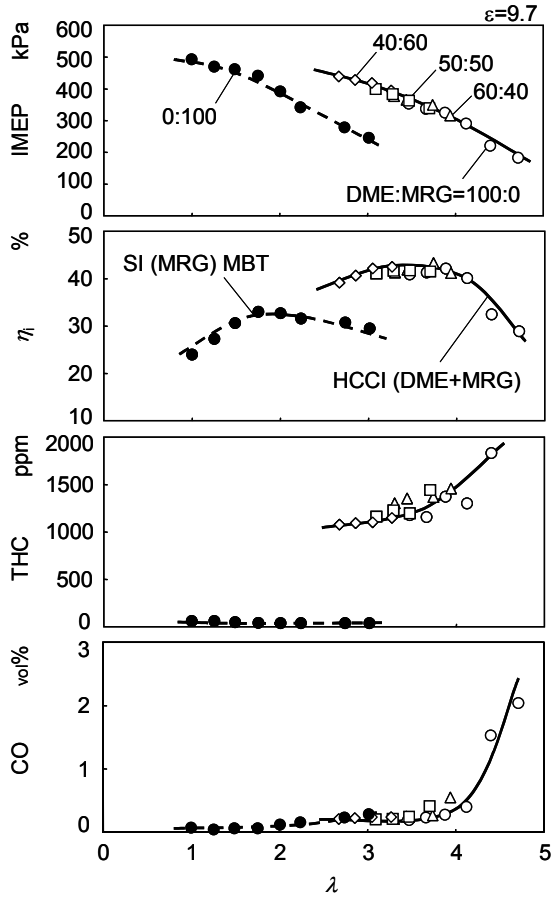


Fig.8 Comparison of SI combustion and HCCI combustion.

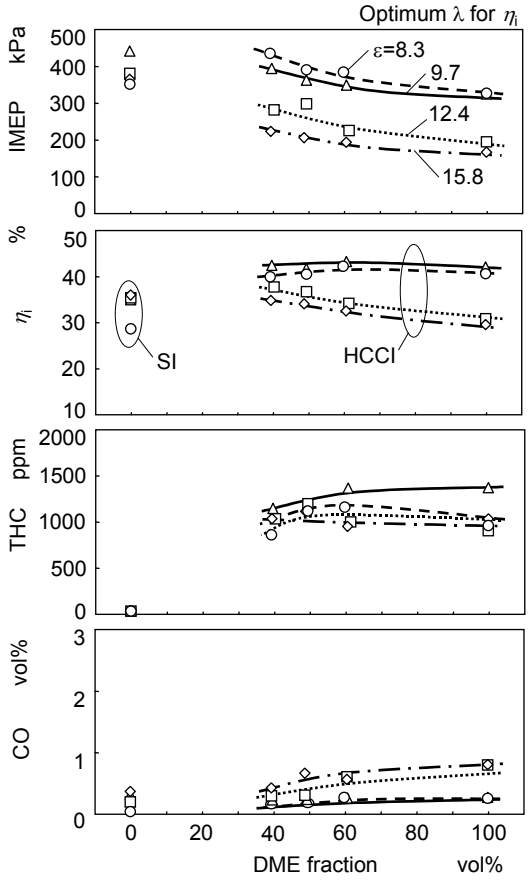


Fig.9 Comparison of SI combustion and HCCI combustion for different compression ratios.

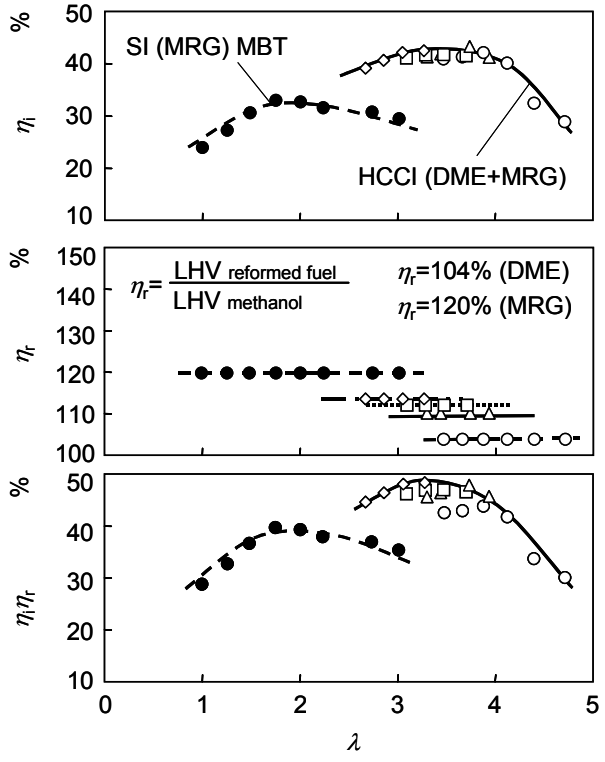


Fig.10 Overall thermal efficiency of HCCI combustion and SI combustion based on methanol.

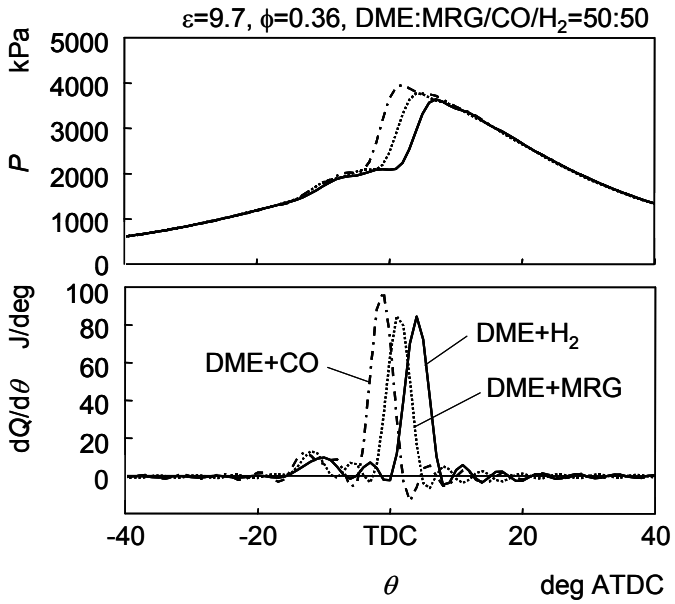


Fig.11 Influences of hydrogen, carbon monoxide and MRG on HCCI combustion of DME.

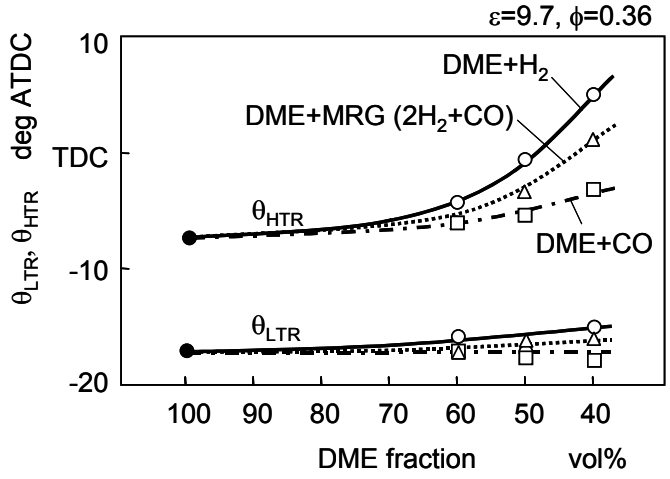


Fig.12 Crank angles at the beginnings of first and second stage heat releases.

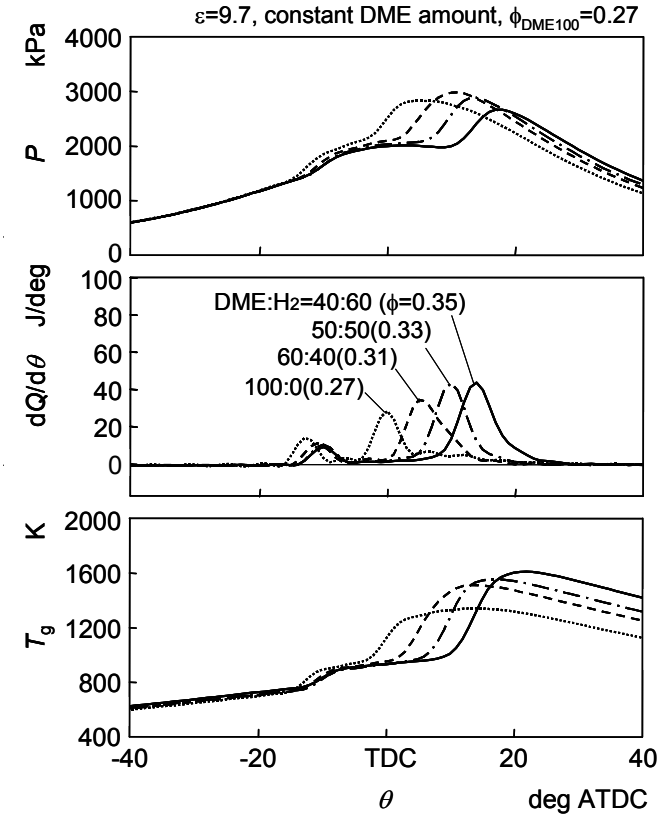


(a) DME and hydrogen

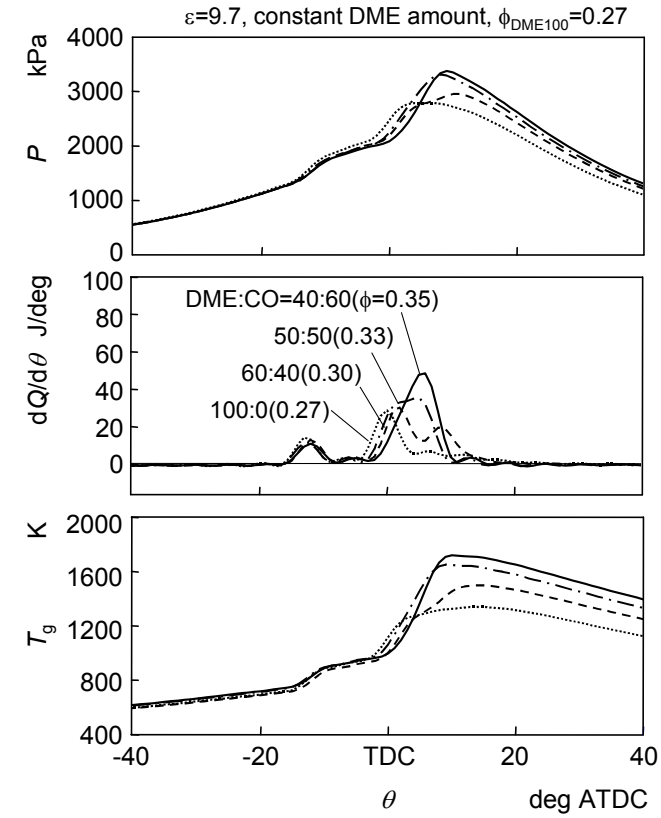


(b) DME and carbon monoxide

Fig.13 Influences of hydrogen and carbon monoxide on HCCI combustion of DME at a constant DME amount.

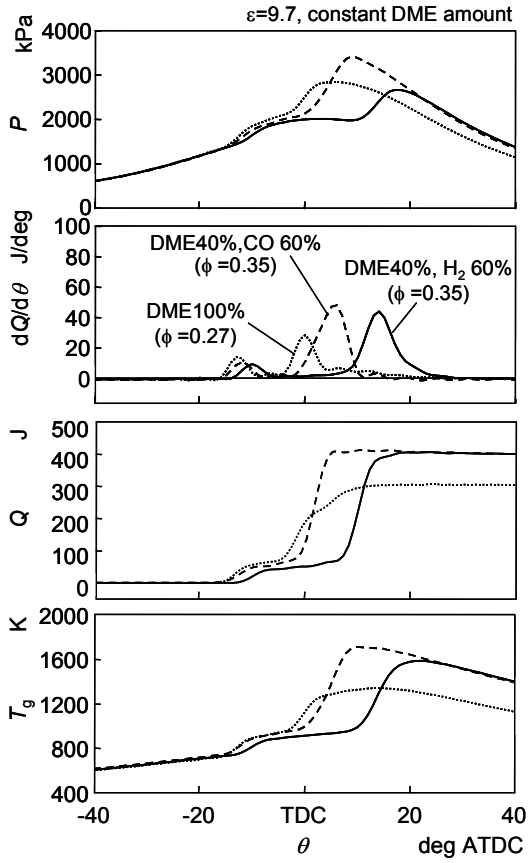


Fig.14 Comparison of effects by hydrogen and carbon monoxide at a constant DME amount.

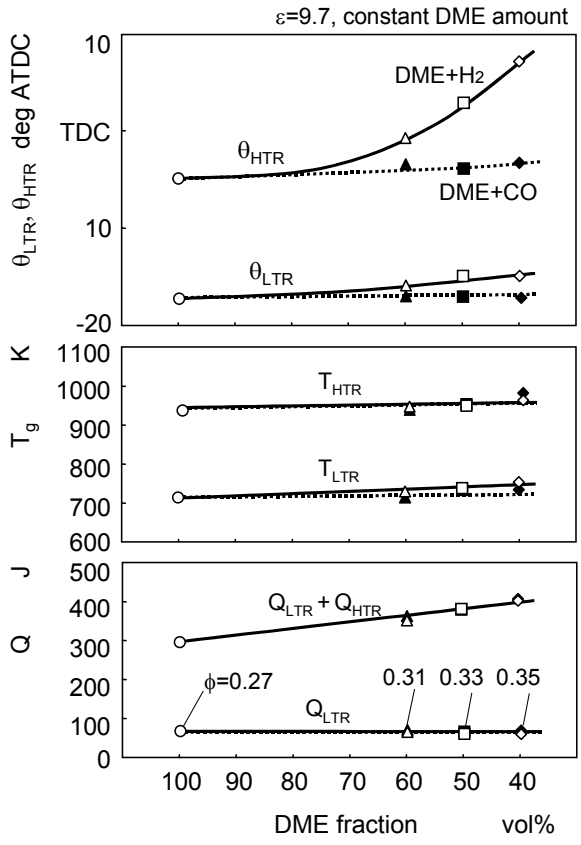


Fig.15 Comparison of effects by hydrogen and carbon monoxide at a constant DME amount.